

Resolved dipole strength below the $E1$ giant resonance in ^{138}Ba

R.-D. Herzberg,^{1,*} C. Fransen,¹ P. von Brentano,¹ J. Eberth,¹ J. Enders,² A. Fitzler,¹ L. Käubler,³ H. Kaiser,² P. von Neumann-Cosel,² N. Pietralla,¹ V. Yu. Ponomarev,⁴ H. Prade,³ A. Richter,^{2,†} H. Schnare,³ R. Schwengner,³ S. Skoda,¹ H. G. Thomas,¹ H. Tiesler,¹ D. Weisshaar,¹ and I. Wiedenhöver^{1,‡}

¹*Institut für Kernphysik, Universität zu Köln, D-50937 Köln, Germany*

²*Institut für Kernphysik, Technische Universität Darmstadt, D-64289 Darmstadt, Germany*

³*Institut für Kern- und Hadronenphysik, Forschungszentrum Rossendorf, D-01314 Dresden, Germany*

⁴*Bogoliubov Laboratory of Theoretical Physics, Joint Institute for Nuclear Research, Dubna, Russia*

(Received 12 July 1999; published 11 October 1999)

The electromagnetic dipole response of ^{138}Ba was measured up to 6.7 MeV excitation energy in a photon scattering experiment. Two Euroball Cluster detectors were used to detect the scattered photons under 94 and 132 degrees. The Cluster at 94 degrees served as a Compton polarimeter. The total observed dipole cross section is in good agreement with previous tagged photon data, but in the present experiment the transition strength and the electric character of most of the transitions has been determined on a state-by-state basis. The data show a concentration of $E1$ strength around 6 MeV. For one of the strongest excitations $M1$ character is suggested. The results of model calculations using the quasiparticle phonon model (QPM) agree with the observed electric dipole strength distribution. [S0556-2813(99)51311-3]

PACS number(s): 21.10.Hw, 23.20.Js, 25.20.Dc, 27.60.+j

The electric dipole response provides a particularly sensitive probe of the structure of nuclei. Due to the repulsive nature of the particle-hole (p-h) interaction, the $E1$ strength is concentrated at high excitation energies of about 10–15 MeV forming the collective giant dipole resonance (GDR), see, e.g., [1]. $E1$ transitions at low energies are significantly modified by the mixture of the elementary p-h excitations with more complex configurations [2,3]. An example, which recently attracted considerable interest, is the transitions to the 1^- members of the multiplet resulting from the coupling of collective quadrupole and octupole phonons in spherical nuclei [4–9]. The delicate interplay of one- (GDR) and two-phonon modes is especially pronounced at and below the particle thresholds. Knowledge of the electric dipole strength in this energy region is therefore an important aspect of nuclear structure whose quantitative description represents a challenge even to advanced models. Experimentally, in the investigation of the γ -ray strength function in the energy region below the GDR, a “bump” in the γ -ray spectra was observed in numerous heavy nuclei [10–15]. This phenomenon is commonly referred to as “pygmy” resonance.

One experimental method especially well suited to studying dipole excitations with good energy resolution and yielding model independent strength and parity information is nuclear resonance fluorescence (NRF); for a detailed review see Ref. [16]. With the advent of the latest generation of high-efficiency compound germanium detectors such as the Euroball Cluster detector [17], the experimental sensitivity has increased significantly [18] and the strength and polarization even of weak transitions can be determined with reasonable accuracy.

The purpose of this Rapid Communication is to report on a NRF experiment performed on the semimagic $N=82$ isotope ^{138}Ba at the superconducting Darmstadt electron linear accelerator S-DALINAC using two composite Cluster detectors. One of them served as a Compton polarimeter in order to determine the parities of the excited levels. A significant amount of $E1$ strength as well as a candidate for a strong $M1$ excitation were found between 5 MeV and the photon end-point energy of 6.7 MeV.

Bremsstrahlung photons were produced in an air-cooled tantalum radiator target and were guided through a 60 cm long lead collimator. The photon scattering target consisted of 3011 mg 99.4% enriched ^{138}Ba sandwiched between boron (627 mg) and aluminum (338 mg) calibration standards of natural composition. The scattered photons were observed by two Cluster detectors located under scattering angles of 94° and 132°. The Cluster detectors were encased in a lead fortress with an average wall thickness of 30 cm to shield them from the highly intense background radiation. Data were taken with the Cologne-Rossendorf FERA Analyzer system which allowed both Clusters to run at 10 kHz singles rate per segment.

The Cluster under 94° was used for measuring the sign of the linear polarization of the scattered γ rays in order to provide parity information on the excited resonance states. Previous experience with polarimetry in NRF experiments has shown that by choosing observation angles slightly larger than 90° the nonresonant background can be reduced significantly while retaining near maximum polarization sensitivity [19,20]. The Cluster detector with its seven large volume Ge crystals has been proven to be an excellent Compton polarimeter [21,22]. Although its segments are not arranged in the usual orthogonal way, numerical simulations [23] as well as experimental tests [21] have shown that the figure of merit for the Cluster’s capability to measure polarizations can be even somewhat larger at high γ -ray energies than that of orthogonal five-crystal arrangements [24] or segmented crystals [19], compensating for the loss of polariza-

*Present address: Oliver Lodge Laboratory, University of Liverpool, Liverpool L69 7ZE, U.K.

†Present address: Wissenschaftskolleg zu Berlin, Wallotstraße 19, D-14193 Berlin, Germany.

‡Present address: Argonne National Laboratory, Argonne, IL 60439.

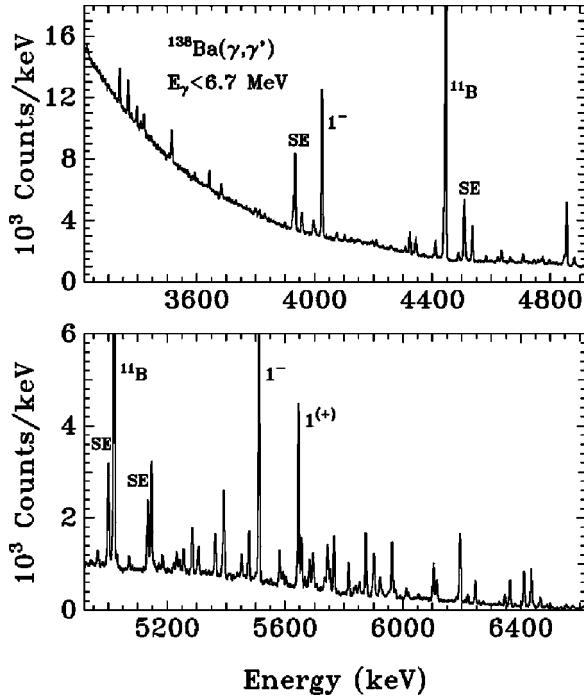


FIG. 1. Top: Total spectrum of the Cluster at 94° from 3.2 to 4.9 MeV. Bottom: The high energy part from 4.9 to 6.6 MeV. Prominent lines labeled ^{11}B result from the calibration standard and SE denotes single-escape lines.

tion sensitivity by its large absolute efficiency. Coincidence spectra were analyzed between perpendicularly adjacent segments (labeled \parallel) and diagonally adjacent segments (labeled \backslash and $/$) with respect to the photon scattering plane. The coincidence asymmetry for the Cluster detector is defined [21] as

$$\epsilon = \frac{I_{\parallel} - 0.5 \times (I_{\backslash} + I_{/})}{I_{\parallel} + 0.5 \times (I_{\backslash} + I_{/})} = \frac{QP}{1 + \frac{1}{3}QP}, \quad (1)$$

where I denotes the coincidence intensity in the coincidence group labeled by the subscript. Each coincidence group contains four detector pairs. Q and P denote the polarization sensitivity of the detector and the linear polarization of the incoming photon with respect to the chosen geometry, respectively. NRF experiments on nuclei with ground-state spin 0^+ lead to maximum polarization $P = \pm 1$ for resonantly scattered photons at 90 degrees according to the positive or negative parity of the resonance state. Therefore, already the sign of the measured asymmetry ϵ uniquely determines the parity of the corresponding excited state.

Figure 1 shows a single spectrum taken at 94° . We observed a total of 58 ground state transitions in ^{138}Ba . Spin quantum numbers were assigned from measured angular correlations. The photon scattering cross sections were measured model independently relative to the well known cross sections in the photon flux calibration standards ^{11}B and ^{27}Al . Effects from nuclear self absorption in the target were taken into account in the evaluation of the cross sections. From the photon scattering cross sections absolute excitation

TABLE I. Excitation energies, spins, parities (whenever an assignment has been possible), experimental asymmetries, branching ratios to the 2_1^+ state, and $B(E1)$ values for those states for which an experimental asymmetry was determined. Excitation strengths above 6 MeV contain asymmetric errors due to an increasing uncertainty of the photon flux calibration.

E [keV]	J^π \hbar	ϵ	Γ_1/Γ_0	$B(E1)\uparrow$ [$10^{-3} e^2 \text{ fm}^2$]
4025.2	1^- ^a	-0.030(19)	0.04(1)	16.7(8)
4322.7	$1^{(-)}$	-0.096(85)	-	2.47(13)
4706.2	1	0.039(111)	-	1.37(8)
4854.1	$1^{(-)}$	-0.064(38)	-	13.1(7)
5145.6	1	-0.024(44)	-	8.6(5)
5283.8	1	-0.038(61)	-	4.07(25)
5391.6	$1^{(-)}$	-0.068(43)	-	10.2(6)
5475.4	1	-0.033(62)	-	4.8(3)
5510.7	1^-	-0.032(17)	0.031(3)	36.7(22)
5581.3	1	-0.018(69)	-	4.5(3)
5644.4	$1^{(+)}$	0.025(30)	0.025(3)	2.52(16) ^b
5654.6	1	-0.043(99)	-	6.6(5)
5694.1	$1^{(-)}$	-0.079(72)	-	5.2(4)
5742.9	1	-0.091(98)	0.10(1)	8.0(6)
5766.1	$1^{(-)}$	-0.062(44)	-	9.5(7)
5814.9	1	-0.013(61)	-	5.1(4)
5873.7	$1^{(-)}$	-0.045(40)	-	12.5(10)
5963.3	1	0.005(40)	-	12.3(11)
6102.7	$1^{(-)}$	-0.062(48)	-	$9.7^{+2.2}_{-1.6}$
6114.1	1	-0.058(73)	-	$5.1^{+1.2}_{-0.9}$
6193.2	1	-0.034(53)	-	$22.8^{+5.6}_{-3.9}$
6244.9	1	-0.016(60)	-	$8.2^{+2.3}_{-1.6}$
6345.6	1	0.034(84)	$0.16^{+0.54}_{-0.15}$	$5.2^{+3.7}_{-1.0}$
6362.4	1	0.019(55)	-	$11.3^{+4.2}_{-2.5}$
6410.3	1	0.023(44)	-	$20.7^{+9.2}_{-5.0}$
6434.1	1	-0.039(44)	-	$21.7^{+10.7}_{-5.4}$

^aParity known from the literature.

^bValue given is $B(M1)\uparrow$ in μ_N^2 (see text).

strengths were deduced. Table I summarizes the results except for weak transitions where the statistical uncertainty of the coincidence signal was too poor for an analysis of the asymmetry.

Figure 2 presents the experimental coincidence asymmetries [cf. Eq. (1)] for ^{138}Ba . Definite parity assignments are indicated by solid circles, tentative assignments by solid squares. The triangles represent the asymmetries of known $E2$ transitions. The open square corresponds to a calibration line which should show no asymmetry. The dashed curves represent the calibrated polarization sensitivity Q of the Cluster detector [21], which is extrapolated above 4.5 MeV. The criteria adopted for assigning parities from the measured asymmetries were as follows. A definite parity assignment was made if the asymmetry was within 1σ of one of the calibration curves, while the other one was excluded by at least 2σ . A tentative assignment was made if the asymmetry was within 1σ of one of the calibration curves, while the other one was excluded by about 1σ . No assignment was made in any other case.

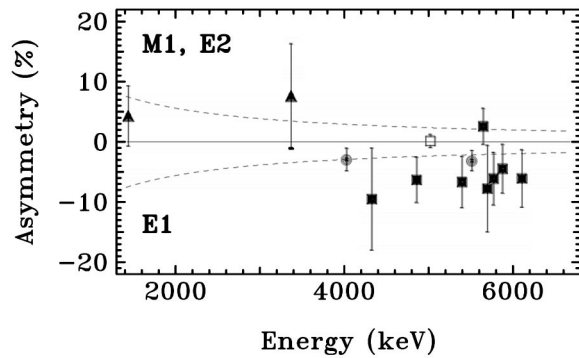


FIG. 2. Experimental asymmetries for γ transitions to the ground state of ^{138}Ba for which at least tentative polarization assignments were made according to the criteria described in the text. Solid circles denote definite, solid squares tentative parity assignments. Triangles correspond to $E2$ transitions. The open square represents the coincidence asymmetry of a calibration line from ^{11}B , which should show no asymmetry. The dashed curves are explained in the text.

The parity assignment can be checked for the strongest transitions in the spectra. The state at 4025 keV decays by a known $E1$ transition [25]. A further check on the quality of the asymmetry data is given by the ^{11}B calibration lines, which should be unpolarized due to the half integer spin values in the odd-mass nucleus. Indeed, the calibration point at 5019 keV in Fig. 2 shows no experimental asymmetry. The two strongest transitions above 5 MeV at 5511 keV and 5644 keV show $E1$ and tentative $M1$ character, respectively, in agreement with the calibration curves. The negative and tentative positive parities of these $J=1$ states were measured for the first time. We assigned two definite and eight tentative parities to the excited states of ^{138}Ba . Note that the analyzing power of the Compton effect for producing polarization decreases towards high energy, e.g., [19]. Meaningful Compton polarimetry in NRF experiments on dipole excitations above 5 MeV is possible only with good statistics, which can be achieved with the highly efficient Cluster detector.

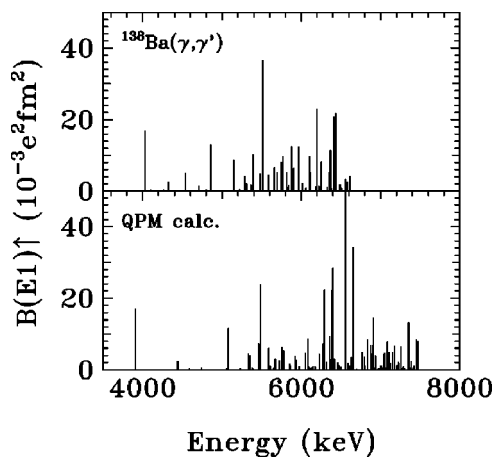


FIG. 3. Top: High resolution $E1$ excitation strength distribution from the present experiment. Bottom: Results of a QPM calculation (see text).

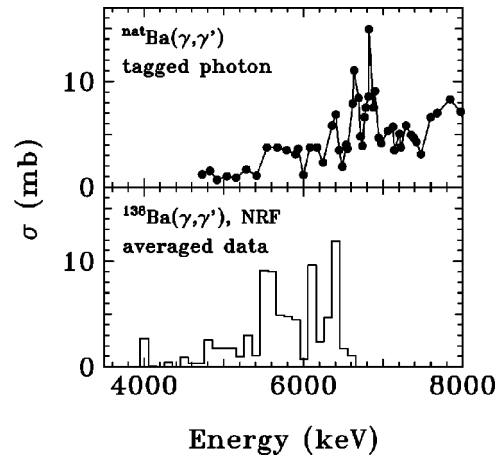


FIG. 4. Top: Elastic photon scattering cross section observed in a tagged photon experiment on a barium target of natural composition [28]. Bottom: Averaged elastic photon scattering cross section calculated from the resolved $B(E1)$ strength distribution of Fig. 3.

The $E1$ strength distribution is shown in the upper part of Fig. 3. The lowest observed $E1$ transition at 4025 keV is the decay of the quadrupole-octupole coupled 1^- state to the g.s. [5,25]. The two-phonon nature of the corresponding states in the $N=82$ isotones ^{142}Nd and ^{144}Sm recently got strong support through (i) the detection of the collective decay branches to the one-phonon states [6,26] and (ii) the close correlation of the $1^- \rightarrow 0_1^+$ with the $3^- \rightarrow 2_1^+$ $E1$ transition strengths between the octupole- and the quadrupole-phonon states [9]. It is, therefore, of interest that we are able to identify the weak $1^- \rightarrow 2_1^+$ decay in ^{138}Ba . Due to the high statistics achieved with the two-Cluster NRF spectrometer a small decay branching ratio of $\Gamma_1/\Gamma_0=3.8(5)\%$ was found. An earlier calculation in the framework of the QPM predicted $\Gamma_1/\Gamma_0=1\%$ for the two-phonon 1^- state in ^{138}Ba [27]. The full calculation discussed below yields $\Gamma_1/\Gamma_0=2.6\%$.

The significant improvement of the data on the $E1$ strength distribution in ^{138}Ba with respect to the previous tagged photon data taken on a barium target with natural isotopic abundance [28] is demonstrated in Figs. 3 and 4. Structure in the elastic tagged photon scattering cross section $\sigma_{\gamma\gamma}(E)$ is hardly visible below 6 MeV (Fig. 4, top). This is in contrast to the new high resolution NRF data (Fig. 3, top), from which we obtain energy-integrated elastic photon scattering cross sections $I_{s,0}(E_x)$ for each resolved resonance state at excitation energy E_x in a model-independent way [16]. In order to compare our data to the tagged photon results we determine averaged elastic scattering cross sections $\sigma_{\gamma\gamma}^{\text{NRF}}(E)=[\sum_E^{E+\Delta E} I_{s,0}(E_x)]/\Delta E$ (Fig. 4, bottom) from the measured individual cross sections $I_{s,0}(E_x)$ in energy intervals $\Delta E=100$ keV. The size of ΔE is close to the energy resolution of the tagged photon experiment [28]. The total elastic photon scattering cross sections between 4.7 MeV and 6.5 MeV derived from both experiments (tagged photon: 55 m barn; NRF: 71 m barn) agree within 25%. Thus, the main part of the tagged photon cross sections in ^{138}Ba comes from the resolved individual transitions and possible contributions

from transitions below our NRF detection limit are small.

The observed $E1$ strength is concentrated between 5 MeV and the end-point energy at 6.7 MeV. Above 6 MeV the extrapolation of the photon flux calibration becomes less reliable resulting in larger and asymmetric uncertainties for the observed strengths given in Table I. The observed $E1$ strengths exceed predictions based on the extrapolation of the GDR towards lower energies [18,29]. A local concentration of $E1$ strength on the tail of the GDR has been observed experimentally in numerous heavy nuclei [10–15]. A variety of theoretical approaches has been put forward to explain this phenomenon. Iachello proposed an interpretation in terms of local breaking of the isospin symmetry [30], which can be extended to the energy regime studied here [31]. It has also been viewed as a vibration of a neutron excess relative to an isospin-saturated core, using density functional theory [32]. RPA calculations with different levels of sophistication also reproduce the local clustering of $E1$ strength, but with somewhat differing conclusions on the underlying particle-hole structure [33–36].

However, none of the above approaches attempts to describe the fine structure resolved here for the first time in ^{138}Ba . Therefore, the theoretical interpretation focuses on QPM calculations including complex configurations up to the coupling of three phonons, which have been highly successful in the description of the $E1$ response near particle threshold in spherical nuclei [14,15]. Free parameters of the interaction were fixed to reproduce the energies and strengths of the lowest collective vibrations (for details see [14,15]). It is worth noting that the GDR is fully included in the model space. So, no renormalization of effective charges has to be introduced [37] in the $E1$ operator in order to obtain a good fit to the data. We use $e_{\text{eff}}^{p(n)} = N(-Z)/A e$, respectively, to separate the center-of-mass motion.

The resulting $E1$ strength distribution is displayed in the bottom part of Fig. 3. The transition to the two-phonon state at 4 MeV is very well reproduced quantitatively when allowing for a destructive interference between the main ($2_1^+ \otimes 3_1^-$) component and a small one-phonon admixture [3], similar to what was found for ^{140}Ce [14] and Sn isotopes [8,38]. The main body of the $E1$ strength is also well reproduced although a one-to-one correspondence is beyond the scope of the model. Similar to the findings in the ^{140}Ce isotope, the distribution is sensitive to the interplay of one- and two-phonon contributions, which lead to an enhancement in the region around $E_x \approx 6$ MeV. The inclusion of three-phonon configurations turns out to be essential for a realistic description of details of electromagnetic strength distributions even at low excitation energies (for another recent example, see [39]). The QPM results suggest the presence of

significant additional $E1$ strength just above the energy interval studied here. Thus, an extension of the experiments towards higher energies would permit an important test of the model predictions.

Finally, we comment on the surprising result of a prominent excitation at 5644 keV with tentative $M1$ character suggested from the polarization analysis. Its strength corresponds to $B(M1) \uparrow = 2.52(16) \mu_N^2$, which is in fact one of the largest $B(M1)$ values observed in heavy nuclei. A possible explanation is an “isoscalar” nature in analogy to similar findings in $^{206,208}\text{Pb}$ [40,41]. It may result from a mixing of the proton and neutron p-h states with high angular momentum, which in a simple two-state model leads by constructive interference to the isovector spin-flip resonance and by destructive interference to an isoscalar transition pushed to lower energies. One should be aware, however, that in a nucleus with significant neutron excess these two modes will be considerably mixed [42]. The nature of these transitions has been found to depend sensitively on mixing outside the major shell, i.e., on the tensor part of the NN interaction. Thus, further confirmation of the magnetic nature of the transition and its unusual strength, e.g., by high-resolution 180° electron scattering [43] would be of high interest.

To summarize, a photon scattering experiment on ^{138}Ba has been carried out using a setup with two Euroball Cluster detectors yielding high resolution data on dipole excitations in ^{138}Ba below 6.5 MeV. One of the Clusters was used as a nonorthogonal Compton polarimeter allowing the determination of parities for several states. A concentration of $E1$ strength riding on the low-energy tail of the GDR is observed. The experimental strength distribution is reproduced well by a QPM calculation including configurations up to the coupling of three phonons. The unexpected observation of a strong transition with likely $M1$ character underlines the importance of state-by-state parity measurements for dipole excitations in this energy region. It would be of considerable interest to extend our knowledge on the fine structure of the electric dipole response towards higher excitation energies. Recent technical improvements of the photon scattering facility at the S-DALINAC [44] open the way for such studies up to excitation energies of about 10 MeV.

We thank F. Iachello, A. M. Oros, R. V. Jolos, A. Gelberg, and P. A. Butler for many stimulating discussions. We are also grateful to the accelerator staff at the S-DALINAC for their support during the beamtime. This work was supported by the BMBF under Contract Nos. 06 OK 862I(O) and 06 DR 666I, by the DFG under Contract Nos. Ri 242/12-2 and Gr 1674/1-1, and by the SMWK under Contract No. 7533-70-FZR/702.

-
- [1] B.L. Berman and S.C. Fultz, *Rev. Mod. Phys.* **47**, 713 (1975).
 [2] K. Heyde and C. De Coster, *Phys. Lett. B* **393**, 7 (1997).
 [3] V. Yu. Ponomarev, Ch. Stoyanov, N. Tsoneva, and M. Grinberg, *Nucl. Phys.* **A635**, 470 (1998).
 [4] F. R. Metzger, *Phys. Rev. C* **14**, 543 (1976).

- [5] R.-D. Herzberg *et al.*, *Nucl. Phys.* **A592**, 211 (1995).
 [6] M. Wilhelm, E. Radermacher, A. Zilges, and P. von Brentano, *Phys. Rev. C* **54**, R449 (1996).
 [7] R. Schwengner *et al.*, *Nucl. Phys.* **A620**, 277 (1997).
 [8] J. Bryssinck *et al.*, *Phys. Rev. C* **59**, 1930 (1999).

- [9] N. Pietralla, Phys. Rev. C **59**, 2941 (1999).
- [10] G.A. Bartholomew, E.D. Earle, A.J. Ferguson, J.W. Knowles, and M.A. Lone, Adv. Nucl. Phys. **7**, 229 (1973).
- [11] R.M. Laszewski and P. Axel, Phys. Rev. C **19**, 342 (1979).
- [12] M. Igashira, H. Kitazawa, M. Shimizu, H. Komano, and N. Yamamuro, Nucl. Phys. **A457**, 301 (1986).
- [13] R. Alarcon, R.M. Laszewski, A.M. Nathan, and S.D. Hoblit, Phys. Rev. C **36**, 954 (1987).
- [14] R.-D. Herzberg *et al.*, Phys. Lett. B **390**, 49 (1997).
- [15] K. Govaert, F. Bauwens, J. Bryssinck, D. De Frenne, E. Jacobs, W. Mondelaers, L. Govor, and V.Yu. Ponomarev, Phys. Rev. C **57**, 2229 (1998).
- [16] U. Kneissl, H.H. Pitz, and A. Zilges, Prog. Part. Nucl. Phys. **37**, 349 (1996).
- [17] J. Eberth, Prog. Part. Nucl. Phys. **28**, 495 (1992).
- [18] P. von Neumann-Cosel, Prog. Part. Nucl. Phys. **38**, 213 (1997).
- [19] B. Schlitt *et al.*, Nucl. Instrum. Methods Phys. Res. A **337**, 416 (1994).
- [20] H. Maser *et al.*, Phys. Rev. C **53**, 2749 (1996).
- [21] D. Weisshaar, Diploma thesis, Universität zu Köln, 1996.
- [22] J. Eberth, Prog. Part. Nucl. Phys. **38**, 29 (1997).
- [23] L.M. Garcia-Raffi, J.L. Tain, J. Bea, A. Gadea, L. Palafox, J. Rico, and B. Rubio, Nucl. Instrum. Methods Phys. Res. A **359**, 628 (1995).
- [24] B. Kasten *et al.*, Phys. Rev. Lett. **63**, 609 (1989); R.D. Heil *et al.*, Nucl. Phys. **A506**, 223 (1990).
- [25] C.P. Swann, Phys. Rev. C **15**, 1967 (1977).
- [26] M. Wilhelm, S. Kasemann, G. Pascovici, E. Radermacher, P. von Brentano, and A. Zilges, Phys. Rev. C **57**, 577 (1998).
- [27] M. Grinberg and Ch. Stoyanov, Nucl. Phys. **A573**, 231 (1994).
- [28] R.M. Laszewski, Phys. Rev. C **34**, 1114 (1986).
- [29] J. Kopecky and M. Uhl, Phys. Rev. C **41**, 1941 (1990).
- [30] F. Iachello, Phys. Lett. **160B**, 1 (1985).
- [31] F. Iachello, Workshop on Low-Lying Magnetic and Electric Dipole Excitations in Nuclei, Darmstadt, 1997 (unpublished).
- [32] J. Chambers, E. Zaremba, J.P. Adams, and B. Castel, Phys. Rev. C **50**, R2671 (1994).
- [33] M. Harvey and F.C. Khanna, Nucl. Phys. **A221**, 77 (1974).
- [34] V.G. Soloviev, Ch. Stoyanov, and V.V. Voronov, Nucl. Phys. **A304**, 503 (1978); **A399**, 141 (1983).
- [35] J.P. Adams, B. Castel, and H. Sagawa, Phys. Rev. C **53**, 1016 (1996).
- [36] A.M. Oros, K. Heyde, C. De Coster, and B. Decroix, Phys. Rev. C **57**, 990 (1998).
- [37] A. Bohr and B. Mottelson, *Nuclear Structure*, Vol. I (Benjamin, New York, 1969).
- [38] K. Govaert *et al.*, Phys. Lett. B **335**, 113 (1994).
- [39] V. Yu. Ponomarev and P. von Neumann-Cosel, Phys. Rev. Lett. **82**, 501 (1999).
- [40] S. Müller, G. Kuchler, A. Richter, H.P. Blok, H. Blok, C.W. de Jager, H. de Vries, and J. Wambach, Phys. Rev. Lett. **54**, 293 (1985).
- [41] M. Schanz, A. Richter, and E. Lipparini, Phys. Rev. C **36**, 555 (1987).
- [42] E. Lipparini and A. Richter, Phys. Lett. **144B**, 13 (1984).
- [43] C. Lüttge, P. von Neumann-Cosel, F. Neumeyer, and A. Richter, Nucl. Phys. **A606**, 183 (1996).
- [44] P. Mohr, J. Enders, T. Hartmann, H. Kaiser, D. Schiesser, S. Schmitt, S. Volz, F. Wissel, and A. Zilges, Nucl. Instrum. Methods Phys. Res. A **423**, 480 (1999).